Supporting Information

Textile Based Capacitive Sensor for Physical Rehabilitation *via* Surface Topological Modification

Liming Chen[a], Mingyang Lu[a], Haosen Yang[c], Jorge Ricardo Salas Avila[a], Bowen Shi[b], Lei Ren[c], Guowu Wei[d], Xuqing Liu[b,*], Wuliang Yin[a,*]

[a] Department of Electrical and Electronic Engineering, University of Manchester, Sackville Street Building, Manchester M13 9PL, United Kingdom.

[b] Department of Materials, University of Manchester, Sackville Street Building, Manchester M13 9PL, United Kingdom.

[c] Department of Mechanical, Aerospace and Civil Engineering, University of Manchester, Sackville Street Building, Manchester M13 9PL, United Kingdom.

[d] School of Computing, Science and Engineering, University of Salford, Salford, M5 4WT, United Kingdom.

*E-mail: xuqing.liu@manchester.ac.uk; wuliang.yin@manchester.ac.uk

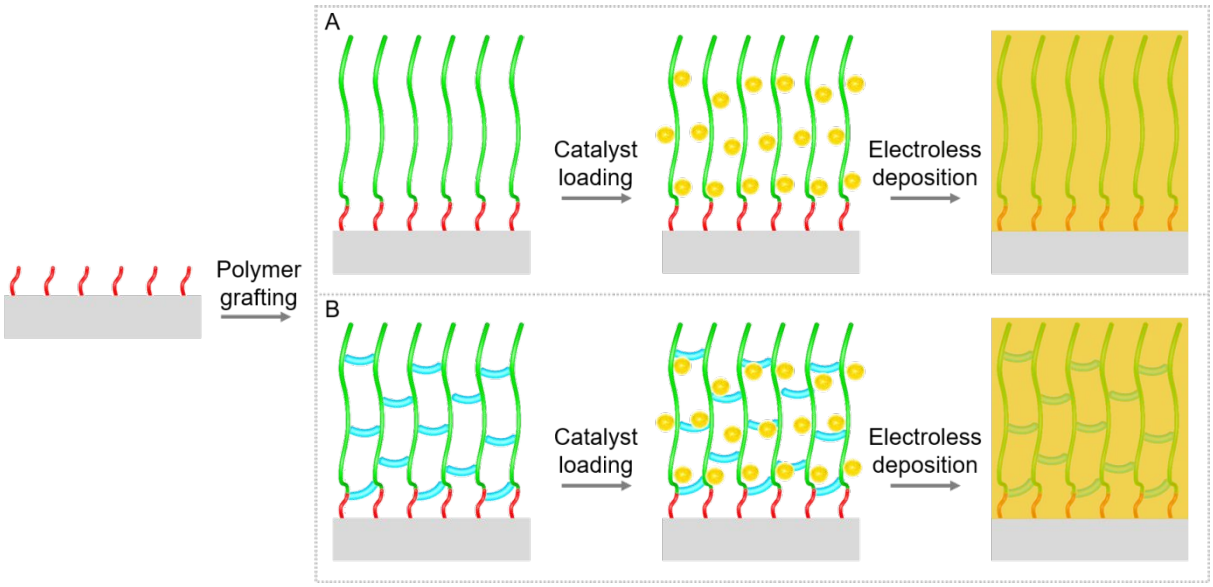

Figure S1. Schematic illustration of the PAMD fabrication, (A) troditional surface-grafted polymer, (B) topologies adhesion of polymer network in this work.

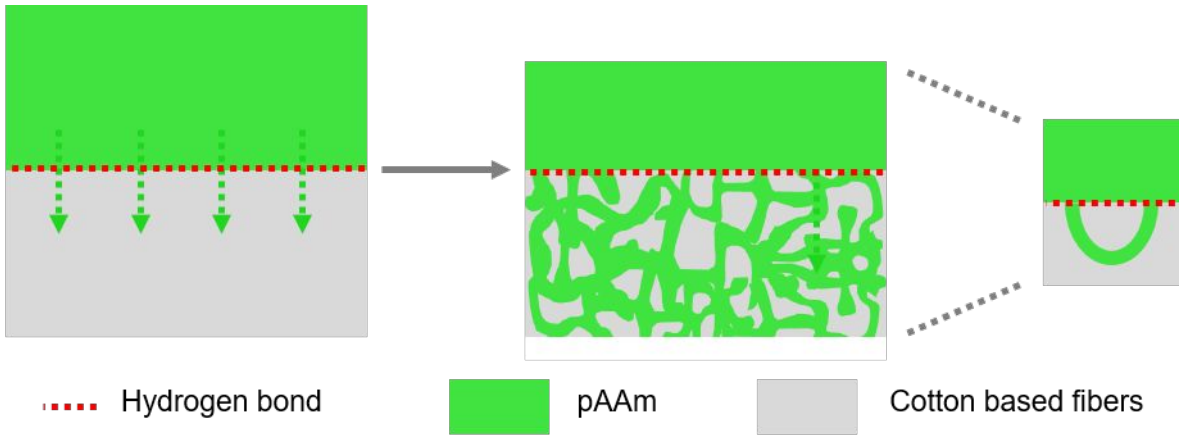

Figure S2. Macroscopic topologies of pAAm adhesion into cotton fibers, (1) thread-hole topology formed between the pAAm and the fibers, (2) bond topology through hydrogen bond formed between amine groups of the pAAm and hydroxyl groups of the fibers.

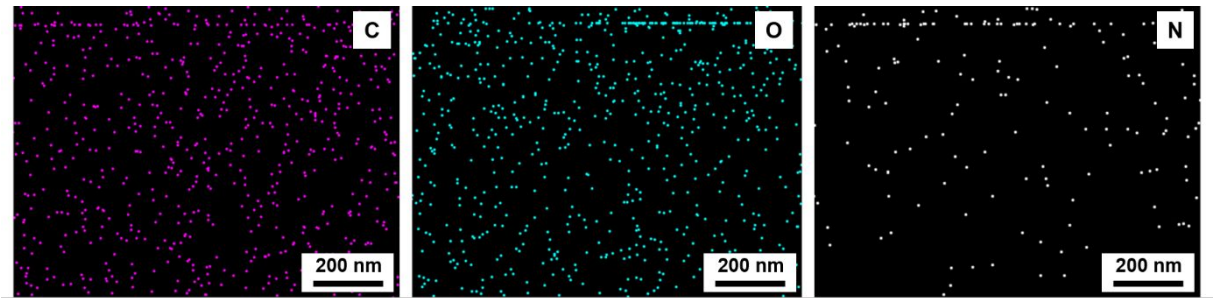

Figure S3. EDS mapping images for carbon, oxygen and nitrogen.

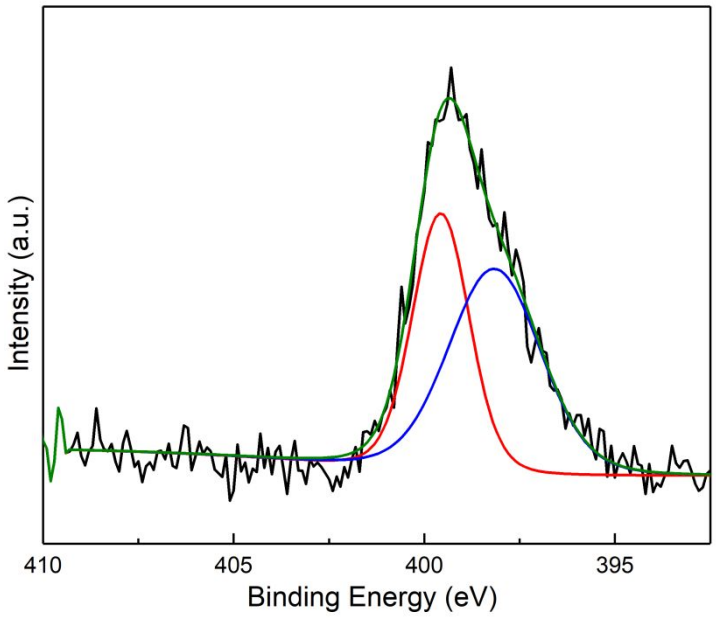

Figure S4. The XPS N 1S spectrum of Pd ion-based fabric.

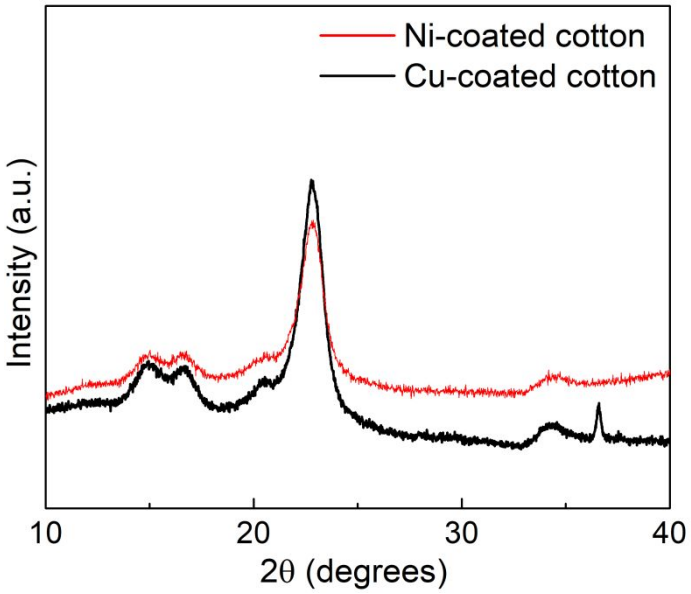

Figure S5. XRD spectrum (10-40 degrees) of (red line) nickel-coated fabric and (black line) copper-coated fabric.

Figure S6. The final state of nickel nanoparticle on the surface of cotton fibers after ELD process.

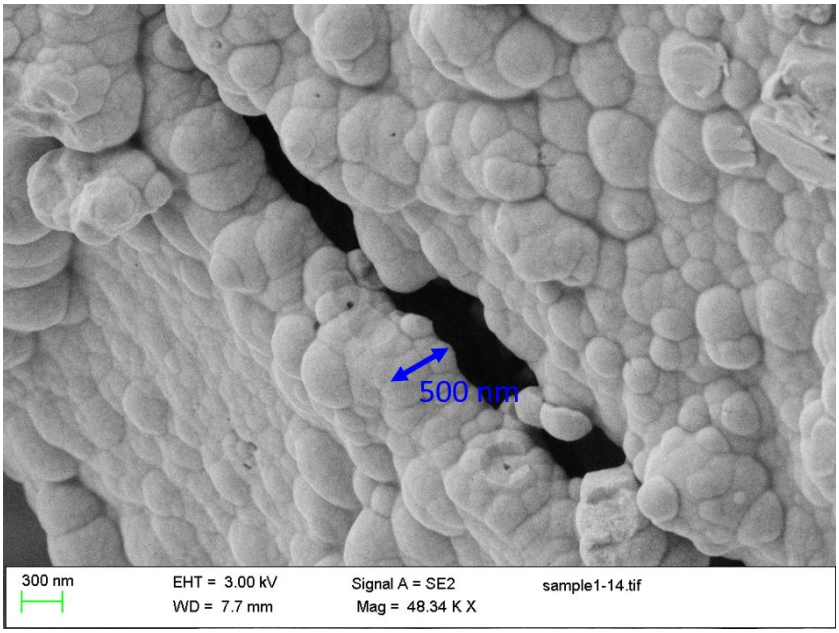

Figure S7. Representative SEM image of the obtained nickel-coated conductive fabrics.

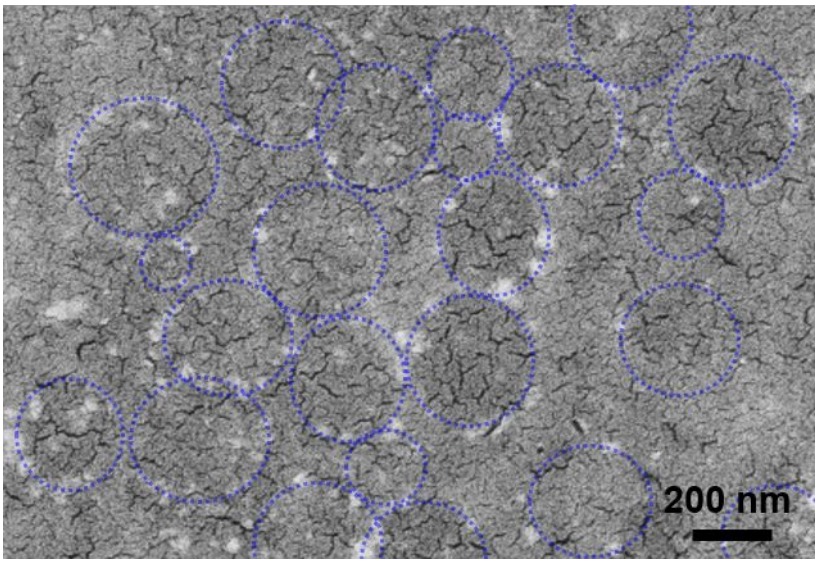

Figure S8. Representative SEM image of the nickel-coated conductive fabrics prepared by 5 min ELD.

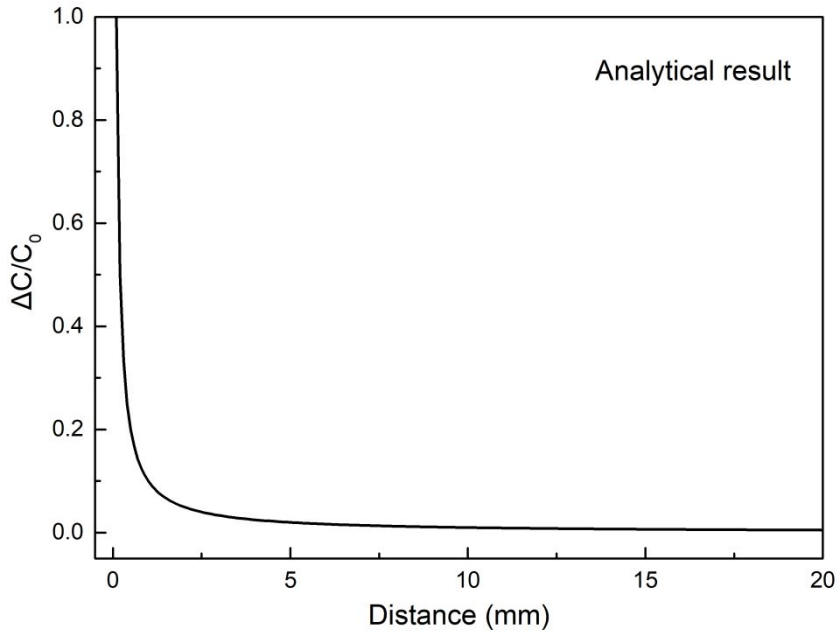

Figure S9. Analytical result for the capacitance changes of conductive sensor as functions of distance.

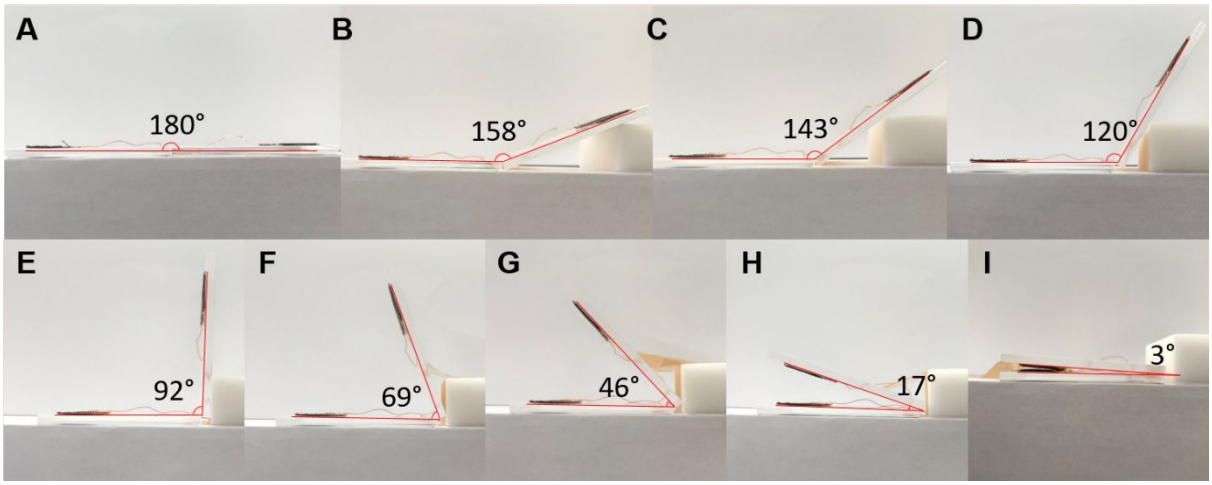

Figure S10. The photos of bending angles measurement.

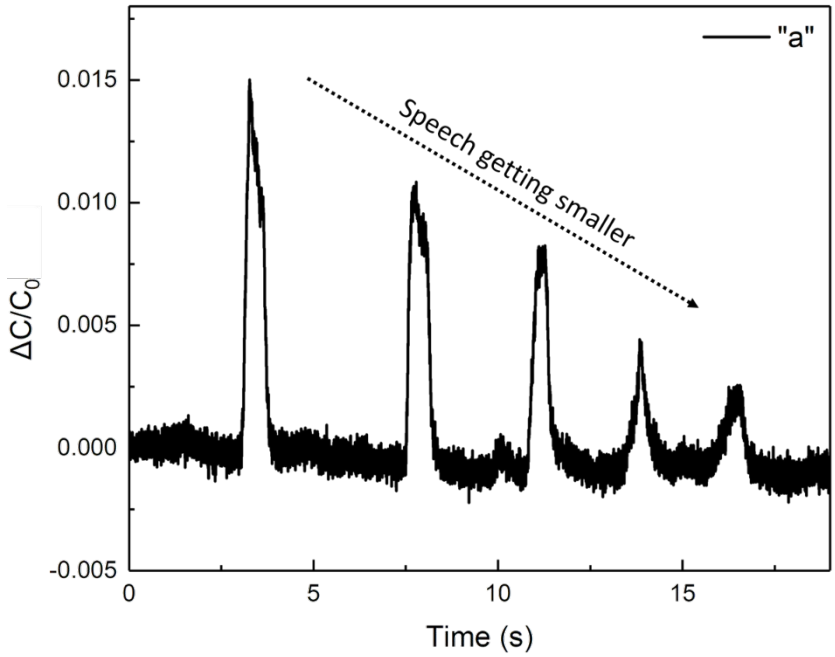

Figure S11. The changes of capacitance as the speech getting smaller.

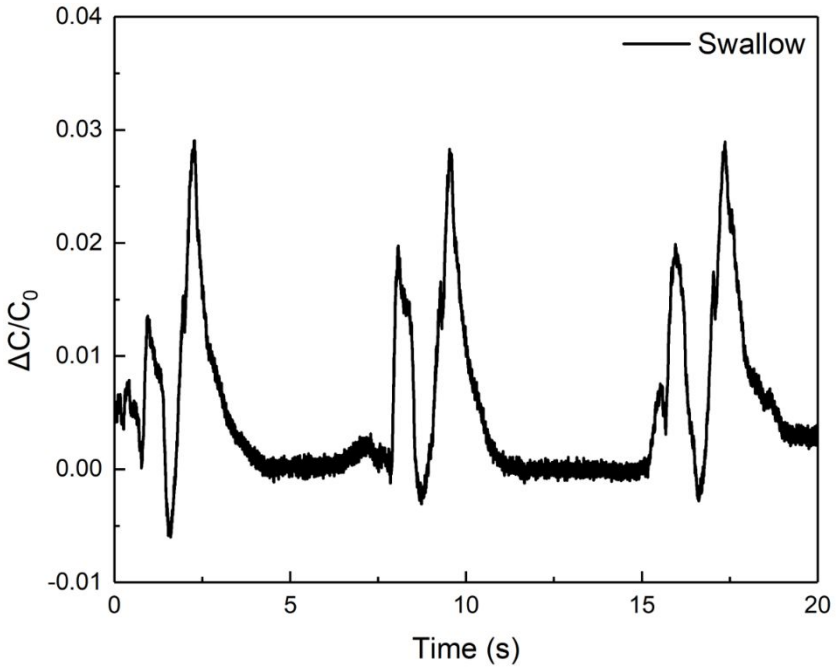

Figure S12. The changes of capacitance as swallowing.

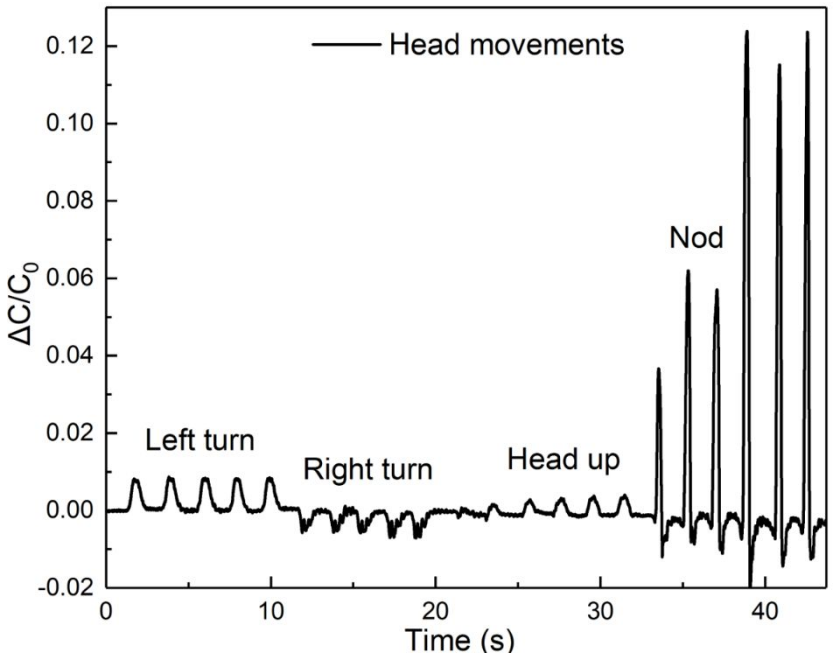

Figure S13. The changes of capacitance as the head movement.

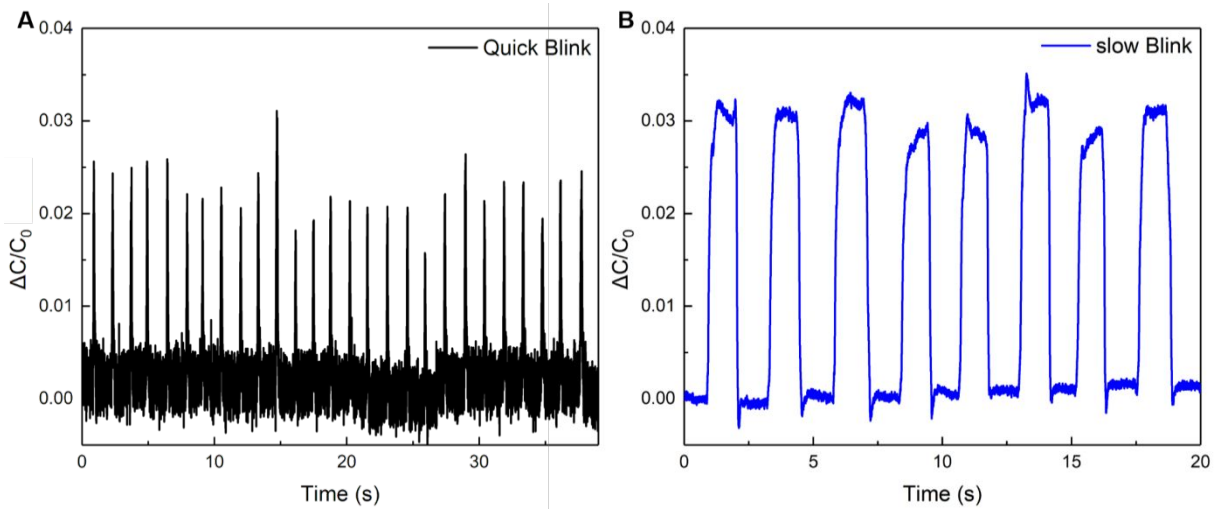

Figure S14. The changes of capacitance as fast and slow blink.

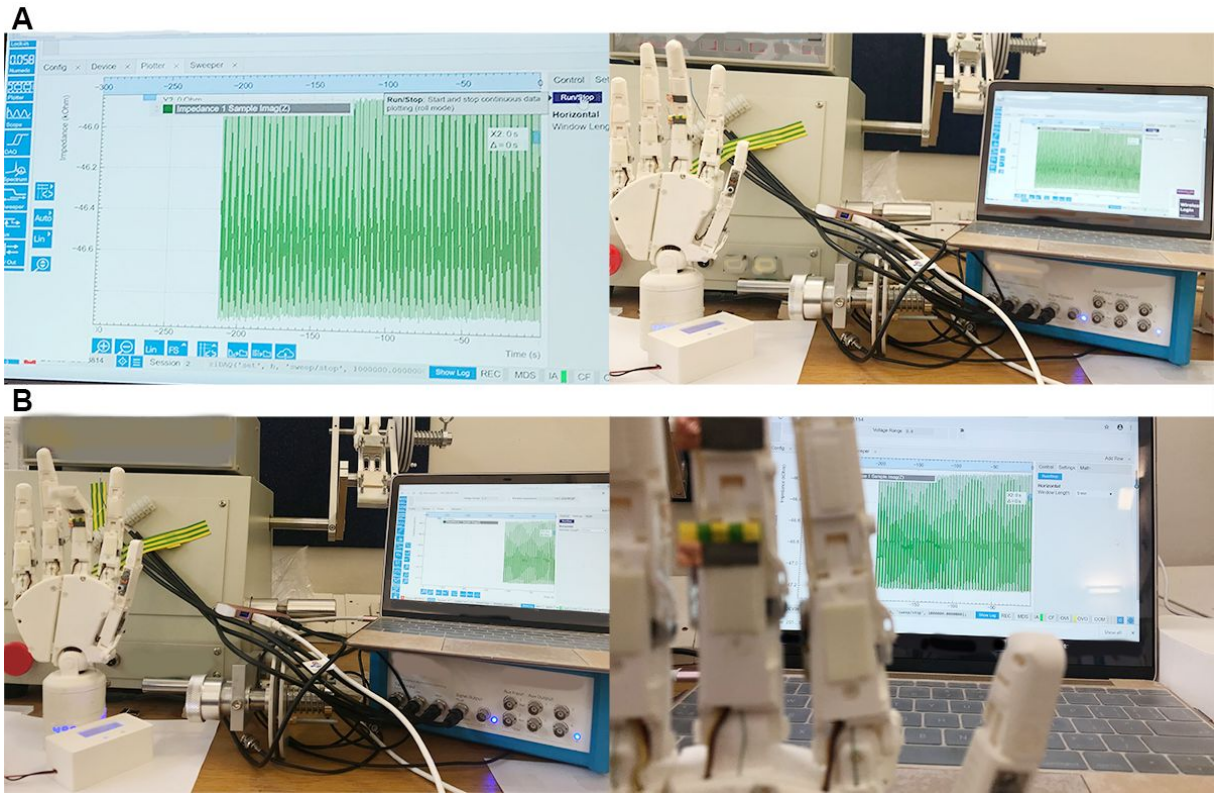

Figure S15. Experimental photos of the repeated finger bending of a MCR-Hand for the test of stability and durability of the sensor.

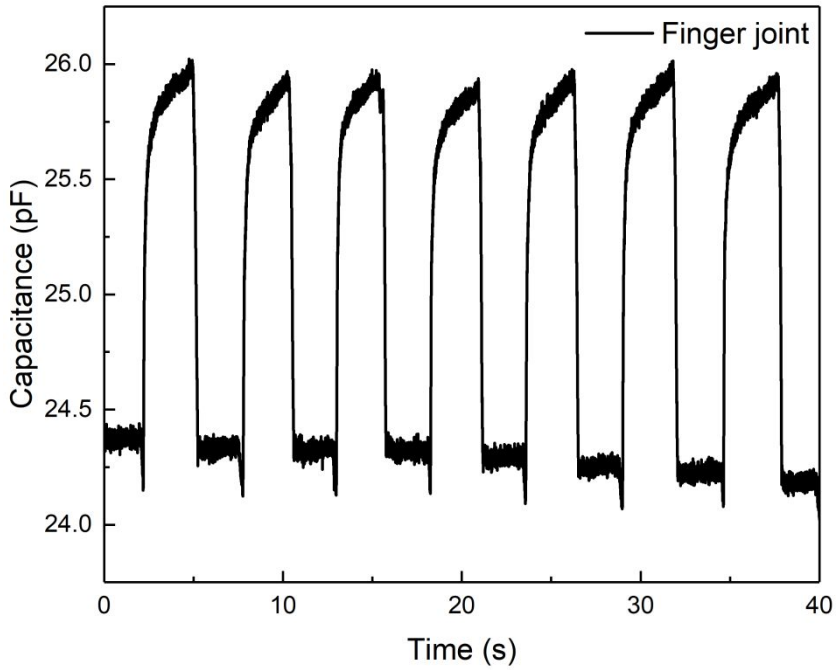

Figure S16. The changes of capacitance absolute value as finger joint bending activities.

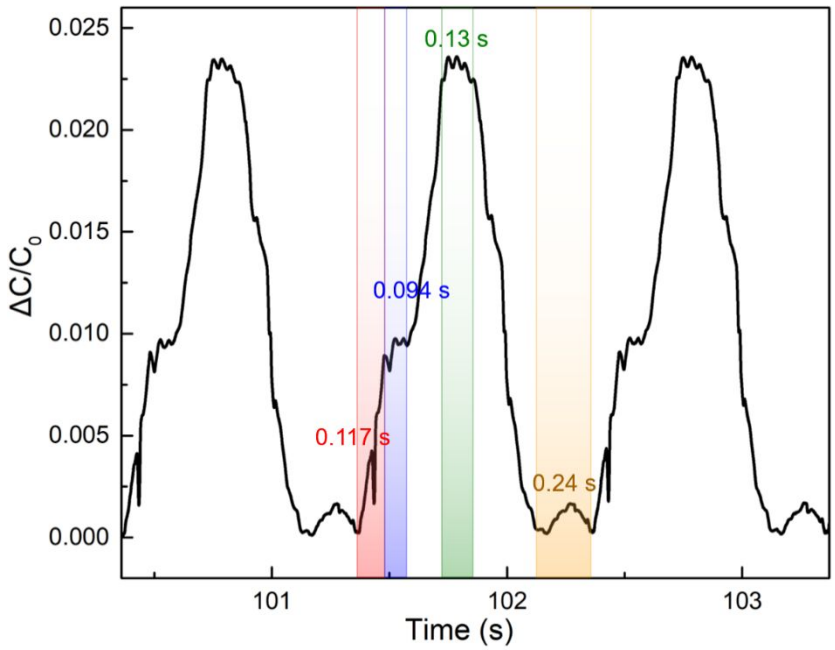

Figure S17. Three cycles of capacitance changes of MCR-Hand finger bending in **Figure 8**.

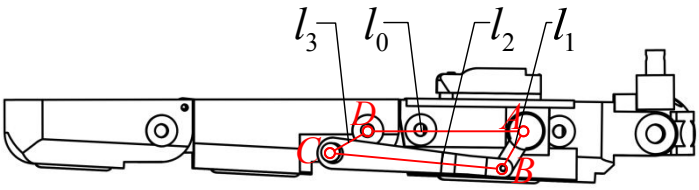

Figure S18. The four-bar mechanism of DIP joint.

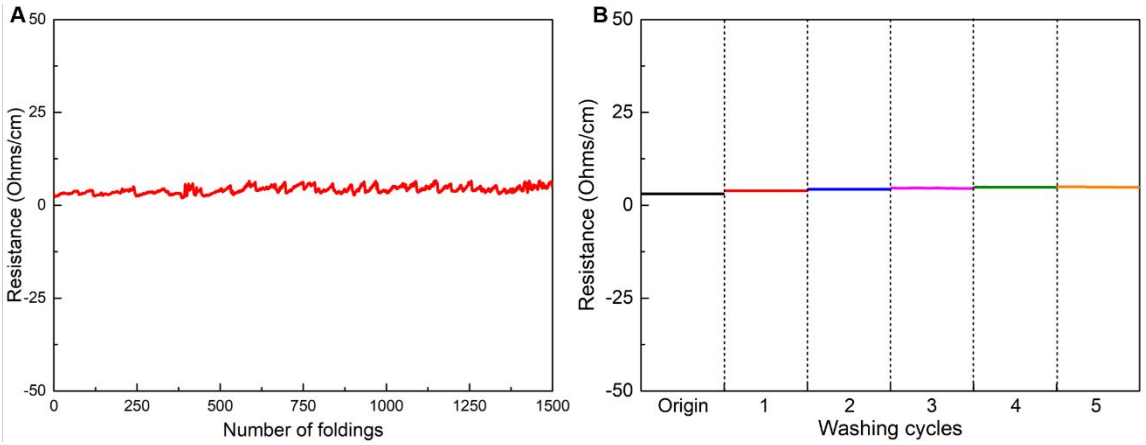

Figure S19. Electrical resistance changes of the prepared conductive nickel-coated fabric for (A) 1500 cycles of folding test, and (B) 5 cycles of washing ability test.

Table S1. Properties of different flexible textile-based sensor reported in the literature.

Ref.	Conductive component	Fabrication strategy	Cost	Conductivity	Sensing Mechanism	Sensitivity	Response time
1	Graphene	Microfluidic spinning	Low	0.5 kΩ	Resistance	$\Delta R/R_0$=15 under 10% strain	
2	Silver nanowire (AgNW)	Screening printing	High		Capacitance	1.62 MPa^{-1} (~1.8 μm)	40 ms
3	Eutectic gallium−indium (eGaIn)	Injection	Low		Capacitance	Tunable	75 ms
4	Silica standard multimode fibers fiber	plane-polished with polymer buffer coating	Low		Light intensity	1.80°	
5	Carbon nanotubes (CNTs)	Spray coating	Low	30 -50 kΩ	Resistance	0.14 rad^{-1}	

6	Single-walled carbon nanotubes (SWCNTs)-filled binary polymer of poly vinylidene fluoride/poly (3,4-ethylenedioxythiophene)-poly (styrenesulfonate) (PVDF/PEDOT:PSS)	Applicator Coating on PET substrate	High	5.8 MΩ	Impedance	90 kΩ/°	~2 s
7	Aluminum	Hot embossing technique	Low		Capacitance	1.15 mm	14 ms
8	Reduced graphene oxide (rGO)	Mixing, directional freezing, freeze-drying, and carbonization	Low	199 **Ω**	Resistance	0.052°	
9	Aluminum and silver	Sputtering technology	High		Resistance and capacitance		164 ms
This work	Nickel/Copper	Electroless deposition	Low	3-5 Ω cm^{-1}	Capacitance	0.2 μm and 0.05°	5 us

Reference

(1) Hu, X.; Tian, M.; Xu, T.; Sun, X.; Sun, B.; Sun, C.; Liu, X.; Zhang, X.; Qu, L. Multiscale Disordered Porous Fibers for Self-Sensing and Self-Cooling Integrated Smart Sportswear. *ACS Nano* **2020**, *14*, 559−567.

(2) Yao, S.; Zhu, Y. Wearable Multifunctional Sensors Using Printed Stretchable Conductors Made of Silver Nanowires. *Nanoscale* **2014**, *6*, 2345−2352.

(3) Yu, L.; Feng, Y.; Tamil Selven, D. S/OM; Yao, L.; Soon, R. H.; Yeo, J. C.; Lim, C. T. Dual-Core Capacitive Microfiber Sensor for Smart Textile Applications. *ACS Appl. Mater. Interfaces* **2019**, *11*, 33347−33355.

(4) Fujiwara, E.; Dos Santos, M. F. M.; Suzuki, C. K. Flexible Optical Fiber Bending Transducer for Application in Glove-Based Sensors. *IEEE Sens. J.* **2014**, *14*, 3631−3636.

(5) Sahoo, B. N.; Woo, J.; Algadi, H.; Lee, J.; Lee, T. Superhydrophobic, Transparent, and Stretchable 3D Hierarchical Wrinkled Film-Based Sensors for Wearable Applications. *Adv. Mater. Technol.* **2019**, *4*, 1900230.

(6) Aziz, S.; Chang, S.-H. Smart-Fabric Sensor Composed of Single-Walled Carbon Nanotubes Containing Binary Polymer Composites for Health Monitoring. *Compos. Sci. Technol.* **2018**, *163*, 1−9.

(7) Sadeghi, A.; Mondini, A.; Totaro, M.; Mazzolai, B.; Beccai, L. A Wearable Sensory Textile-Based Clutch with High Blocking Force. *Adv. Eng. Mater.* **2019**, *21*, 1900886.

(8) Zhuo, H.; Hu, Y.; Tong, X.; Chen, Z.; Zhong, L.; Lai, H.; Liu, L.; Jing, S.; Liu, Q.; Liu, C.; Peng, X.; Sun, R. A Supercompressible, Elastic, and Bendable Carbon Aerogel with Ultrasensitive Detection Limits for Compression Strain, Pressure, and Bending Angle. *Adv. Mater.* **2018**, *30*, 1706705.

(9) Atalay, O.; Atalay, A.; Gafford, J.; Wang, H.; Wood, R.; Walsh, C. A Highly Stretchable Capacitive-Based Strain Sensor Based on Metal Deposition and Laser Rastering. *Adv. Mater. Technol.* **2017**, *2*, 1700081.